Journal of Power Sources 629 (2025) 236010

Contents lists available at ScienceDirect

Journal of Power Sources

journal homepage: www.elsevier.com/locate/jpowsour

Designing, building and operating an up-scaled methane producing bioelectrochemical system for power-to-methane

Micaela Brandão Lavender [a,b,1], Jos Steller [b,1], Dandan Liu [b,2], Rieks de Rink [b], Shiba Tofik [b], Annemiek ter Heijne [a,*]

[a] *Environmental Technology, Wageningen University and Research, Bornse Weilanden 9, Wageningen, 6708 WG, The Netherlands*
[b] *Paqell B.V., Reactorweg 301, Utrecht, 3542 AD, The Netherlands*

HIGHLIGHTS

- A 17 L methane producing BES with GAC as cathode material was built.
- Stable performance was observed for 400 days with an energy efficiency of around 40%.
- Methane production rates up to 280 NL $m^{-3}{}_{BES}$ d^{-1} were achieved.

GRAPHICAL ABSTRACT

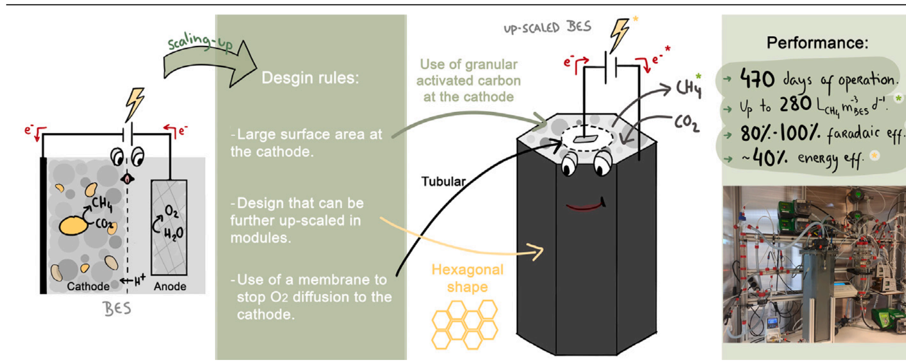

ARTICLE INFO

Keywords:
Scaling up
Power-to-methane
Bioelectrochemical system
Granular activated carbon
Hexagonal prism shape

ABSTRACT

A 17 L scale up methane producing bioelectrochemical system (BES) for power-to-gas application was built taking into account: (1) use of granular activated carbon as cathode material to provide a large surface area for the reaction to take place; (2) a commercially available tubular membrane separating the anaerobic cathodic reaction from the anodic oxygen production; (3) an hexagonal prism design that can be further up-scaled in modules, specially avoiding the hurdle of producing electrodes in non-commercially available sizes. The BES was operated for 470 days with step wise increase in applied current density between −6 and −125 A $m^{-3}{}_{BES}$, with resulting methane production rates between 10 NL $m^{-3}{}_{BES}$ d^{-1} and 280 NL $m^{-3}{}_{BES}$ d^{-1} and faradaic efficiency ranging between 80% and 100%. A stable performance was observed after a start-up period of around 70 days. Furthermore, changes in the electrolyte composition and anode dimensions were made in order to decrease losses associated to the electrolyte and anode reaction, respectively. The distribution of the voltage losses is assessed in this paper and for the majority of the experimental time the energy efficiency ranged around 40%, specifically when operating with an electrolyte with Na^+/K^+ carbonate/bicarbonate concentrations of 0.2 M, 0.4 M and 0.6 M and with an anode surface area equal to or larger than 0.02 m^2. Besides the BES itself, the reactor line-up included a bubble column, an oxygen stripping unit and an interchange vessel, all of which essential for its operation.

* Corresponding author.
E-mail address: annemiek.terheijne@wur.nl (A. ter Heijne).
[1] Shared first authorship.
[2] Lead contact.

https://doi.org/10.1016/j.jpowsour.2024.236010
Received 1 October 2024; Received in revised form 25 November 2024; Accepted 2 December 2024
Available online 12 December 2024

1. Introduction

According to the International Renewable Energy Agency, a key barrier in the energy transition is infrastructure, namely (1) limited electricity transport infrastructure (grid), (2) limited electricity storage infrastructure, (3) insufficient adaptation of other distribution infrastructure, such as gas pipelines, and (4) unfitness of end-users, such as households, for electrification. [1] Power-to-methane in a bioelectrochemical system (BES) is an electricity storage technology, alternative to the ones readily available, that can help bypass the presently unprepared infrastructure. In a methane producing BES, carbon dioxide (CO_2) is biologically reduced to methane (CH_4) at the cathode. The electrons needed to drive this reaction are made available through oxidation of water to oxygen at the anode and the consumption of electrical power. Hence, the process converts electrical energy into chemical energy in the form of methane. Methane as a gaseous chemical energy carrier allows for long term and stable storage, and is more energy dense than its alternative, hydrogen, at the same pressure. Moreover, methane as an end product can be transported and stored using the currently existing gas infrastructure, including pipelines, and can serve non-electrified households. Hence, Power-to-methane in BES offers an alternative that can be easily implemented within the currently existing infrastructure, in comparison to other power-to-gas alternatives.

However, BESs need to be up-scaled before implementation is possible and up-scaling BESs faces a number of challenges, (1) materials and designs that provide effective large surface areas and good microbe-material interactions are needed in order to achieve high volumetric reaction rates, (2) increasing size normally results in increased distances between electrodes and this results in increasing diffusion limitations, hence larger the energy losses, (3) the design for scaling-up is largely dependent on application, hence they need to be function-oriented. [2–6] So far, most efforts have focused on researching and summarizing scaling-up strategies for waste water treatment applied BESs. [3,4,7,8] However, there are a few studies on scaling-up BES for power-to-gas applications, with either hydrogen as an end product, [9,10] or, more recently, methane. [11–15] However, in the latter studies, either low methane production rates or low energy efficiencies were observed.

The goal of this study was to (1) design an efficient BES both in terms of rates and energy use with focus on application as a power-to-methane technology, and to (2) operate the system for long term and analyze its performance over time.

Design considerations

The main consideration taken into account when creating the scale up BES design were: (1) the use of materials that are commercially available, experience low losses and have large surface areas (specially at the cathode), (2) the use of a membrane separating the anode and cathode, whilst allowing for easy maintenance, and (3) a final design that can be further scale up in modules.

The use of granular activated carbon (GAC) as cathode material in laboratory scale methane producing BES has resulted in low cathode overpotential [16]. Moreover, GAC has a larger surface area available for the attachment of microorganisms, in comparison to flat plate electrodes. GAC is also thermally stable material, resistant to corrosion and relatively low in costs, which is relevant for large scale implementation. Although these are promising characteristics, the questions remains on how to scale up efficiently using this 3D electrode. For this, the GAC had to be tightly packed between the membrane and the current collector. For the anode current collector, a commercially available Iridium-Ruthenium coated Titanium electrode was used, since it is state of the art for water oxidation.

A membrane-less configuration is often considered when scaling up BESs in order to avoid diffusion-associated losses across the membrane, and to reduce costs, specially those associated to maintenance of the membrane. [2,6,17] However, in a methane producing BES, a membrane-less design is not a good option taking into account the anaerobic nature of the biological reduction reaction at the cathode, and the formation of oxygen at the anode. Hence, a commercially available cation exchange tubular shaped membrane was centered in the BES. The tubular shape of the membrane allows it to be more easily removed, provided that between the membrane and the GAC bed a meshed plastic spacer is added, keeping the pressure on the GAC against the current collector when removing the membrane.

Scaling up in modules is currently an important concept that has been under consideration to a large extent in designing BES. [2,4] Modular-friendly designs allow the system to be further scale up at any point in time and without compromising rates which are associated to the design. A. Wang, et al. 2020, designed a flat plate BES that can be scale up in modules by alternating plates. [6] The uniqueness of the design laid on the fact that the flat plates were slightly bent and when stacked they would create the pattern resembling a honeycomb. Hence, merging the concept of a modular flat plate electrode design with a tubular flow-through design. Inspired by this, the current collector was shaped forming an hexagonal prism (see Section 2.1, Fig. 1). One side of the hexagonal prism of one BES can be in contact with another side of another hexagonal BES, and so on, mimicking a honeycomb. In this way allowing current to be distributed through the different modules (BES). This would not be possible if the outside current collector was tubular shaped. For more details on the experimental design check Section 2.1.

Operation and evaluating performance

This work assesses the performance of and up-scaled methane producing BES in terms of methane production rates and energy efficiency during an operational period of 470 days. Moreover, a comparison is made with other power-to-gas BES designs that are larger than 17 L. Lastly, opportunities and challenges of the design in this work are discussed.

2. Methods

A 17 L bioelectrochemical system (BES) was built, operated and its performance was analyzed. Accordingly, the reactor design (Section 2.1), operational parameters (Section 2.2) and the analysis conducted in this work (Section 2.3) are extensively laid out in this section.

2.1. Reactor design

2.1.1. Bioelectrochemical system

A schematic representation of the hexagonal prism shaped BES and the materials used are shown in Fig. 1, including the dimensions of the BES. The hexagonal housing was made of PVC and a tubular cation exchange membrane (CE-2, RisingSun membrane technology, Beijing, China) with a projected surface area of 0.12 m^2 was centered separating the anode chamber inside (3 L) from the cathode chamber outside (14 L).

The cathode chamber contained a current collector and a granular activated carbon (GAC) packed bed. The current collector was stainless steel mesh with projected surface area of 0.34 m^2. GAC (Norit® PK 1–3, Cabot Norit activated carbon, Amersfoort, The Netherlands) with a bulk density of 290 kg m^{-3} was used as cathode electrode material and filled the entire volume of the cathodic chamber with exception of a small thin layer at the bottom (6.5 cm in height) which was filled with glass beads in order to ensure good liquid distribution. Around the tubular membrane, a fiberglass (PTFE) mesh with the pore size of 1.1 mm × 1.3 mm and a layer of graphite felt attached with carbon string were placed to ensure no damage to the membrane due to the GAC. Good compactness of the GAC bed is important to ensure contact between current collector and granule bed, as confirmed by measuring

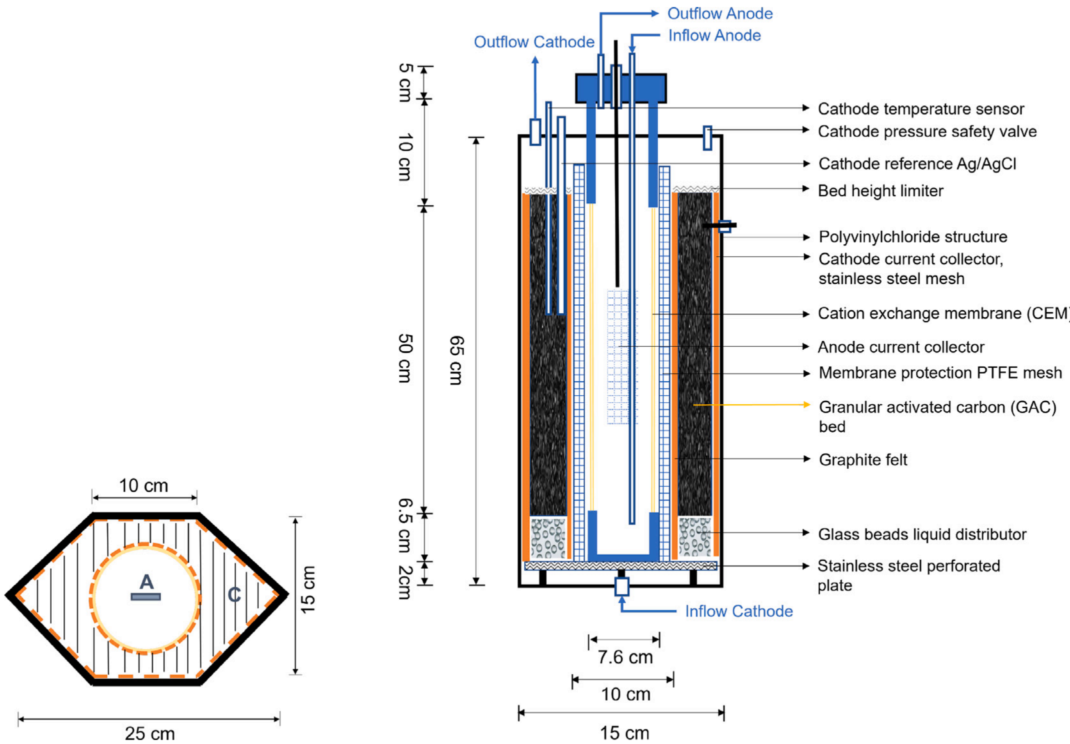

Fig. 1. Schematic representation of the scale up BES from above (left), and of the interior from a side perspective (right), with indication of the different components and sizes.

the capacitance, which was 363 F g^{-1}. At the top of the GAC bed, an Ag/AgCl (in 3M KCl) reference electrode was placed. All potentials are reported vs. this Ag/AgCl reference electrode (equivalent to −0.29 V vs. SHE).

The anode chamber contained an Iridium-Ruthenium coated Titanium meshed electrode (Baoji Zhufeng Metal Processing Co., Ltd., China) that was bent into a cylindrical shape and had a projected surface area of 0.01 m^2. At day 147, an Ag/AgCl reference electrode (in 3M KCl) was also inserted in the anode chamber. To test the size of the anode electrode on the losses associated to the anodic reaction the surface area of the anode electrode was increased 2, 5 and 10 times throughout the run.

2.1.2. Set-up

The BES was connected through a series of liquid flows to the rest of the reactor set-up, which consisted of a bubble column, an oxygen stripping unit and an interchange vessel as shown in Fig. 2. The catholyte was recirculated between the cathode chamber, the bubble column and the interchange vessel. The anolyte was recirculated between the anode chamber, the oxygen stripping unit and the interchange vessel.

The bubble column had a total volume of 4.3 L and dimensions of 6 cm × 160 cm (diameter × height). In the bubble column, CO_2 gas was sparged in counter flow to the electrolyte flow at a rate of approximately 2.1 L h^{-1}. The CO_2-rich electrolyte was then circulated to the cathode, via pump P2. The electrolyte at the outlet of the cathode was separated in two flows, with a glass T-piece, one to the top of the bubble column and the other one recirculated back to the cathode, via P1. The glass T-piece allows the separation of the formed gas from the electrolyte, and directs it to the bubble column. P1 was used for internal recirculation of the electrolyte over the cathode chamber.

The oxygen stripping unit had a total volume of approximately 0.8 L and dimensions 3 cm × 81 cm (diameter × height). In the oxygen stripping unit, N_2 gas was sparged in counter flow to the electrolyte flow at a rate of 5.1 L h^{-1}. The electrolyte coming from the anode chamber was circulated to the oxygen stripping unit, by P4, so that the produced oxygen from the BES was stripped away before the electrolyte was circulated back to the anode. Before starting experiments it was observed that an hydraulic retention time (HRT) of 1 min is sufficient to remove at least 90% of the produced O_2.

The interchange vessel had the purpose of mixing together the electrolyte recirculating through the cathode chamber and electrolyte recirculating through the anode chamber. The interchange vessel could hold up to 3.4 L of electrolyte. Throughout operation of a BES, specially at haloalkaline conditions, cations can be transported across the cation exchange membrane from the anode to the cathode to balance the transport of electrons from the anode to the cathode. As a result, the conductivity of the catholyte can increase and the conductivity of the anolyte can decrease. Therefore, mixing anolyte and catholyte was used as a strategy to keep the conductivity of the catholyte and the anolyte constant. This constant conductivity was needed in order to keep the system stable, which becomes especially important for long term operation. The electrolyte recirculating through the cathode chamber would overflow to the interchange vessel with the use of a level control overflow system in the bubble column (LC, see Fig. 2), and the electrolyte recirculating through the anode chamber would overflow to the interchange vessel from the oxygen stripping unit. The (mixed) electrolyte in the interchange vessel would then be pumped to the cathode chamber via pump P3, and to the anode chamber via pump P4. For simplicity, throughout the paper we call this the "interchange strategy". Appendix A summarizes when the interchange strategy was used. Note that the interchange strategy was not used from day 0 (start-up, see Section 2.2) up to day 51.

2.2. Reactor operation

2.2.1. Inocula

The set-up was inoculated (at day 0) with 2L anaerobic granular sludge from an up flow anaerobic sludge blanket (UASB) reactor. This UASB treats papermill wastewater and was located in Eerbeek (The Netherlands). The granular sludge was grinded into flocculent sludge

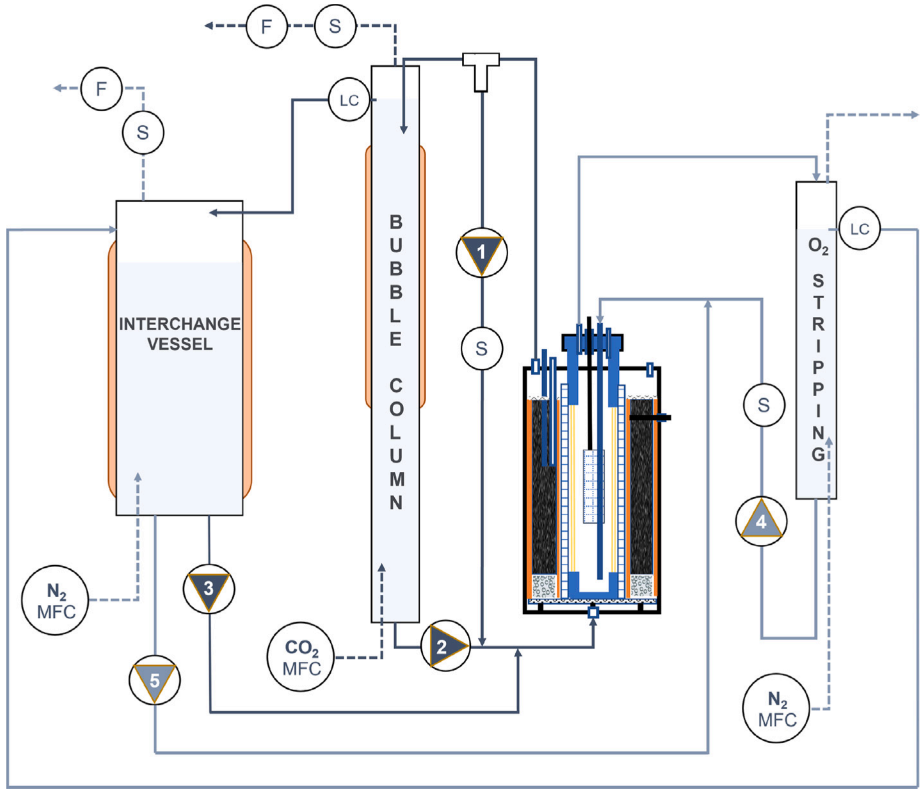

Fig. 2. Schematic overview of the experimental set-up, including interchange vessel, bubble column, BES cell and oxygen stripping unit from left to right. The dark colored lines represent the cathode recirculation, the light colored lines represent the anode recirculation; the dashed lines represent the gas flows. F stands for flow meter, S stands for sampling point (both liquid and gas), LC stands for level controller (though overflow), and MFC stands for mass flow controller (both for CO_2 and N_2). (For interpretation of the references to color in this figure legend, the reader is referred to the web version of this article.)

with a disperser (IKA T25 digital ULTRA-TURRAX) and then washed with tap water before addition to the set-up to remove organics in the liquid phase. The total volatile suspended solids (VSS) of the washed sludge was 50.77 ± 5.47 g L^{-1}.

2.2.2. Electrolyte

Initially, up to day 100, the system was operated under "standard conditions", mimicking the previous work on laboratory scale methane producing BES. [16,18] This standard medium consisted of 50 mM phosphate buffer (13.6 g L^{-1} KH_2PO_4 and 56.7 g L^{-1} Na_2HPO_4) with 0.3 g L^{-1} NH_5CO_3, 1 mL L^{-1} Wolfe's vitamin solution, [19] and 1 mL L^{-1} Wolfe's mineral solution. [19] At the anode, the same buffer solution was used but without the addition of ammonium, vitamin and minerals.

At day 100, the alkalinity of the electrolyte was increased to 0.2 M with bicarbonate electrolyte by adding both $NaHCO_3$ and $KHCO_3$ at a 4:1 ratio. Additionally, 0.3 g L^{-1} NH_4HCO_3, 1 mL L^{-1} Wolfe's vitamin solution, [19] 1 mL L^{-1} Wolfe's mineral solution, [19] 6.78 mg L^{-1} of $MgSO_4x7\,H_2O$ and 3.99 mg L^{-1} of $Na_2HPO_4x2\,H_2O$ were added to the electrolyte we refer to as "haloalkaline electrolyte". Under the same applied current density, the alkalinity of the electrolyte was further increased in the same manner as described above to 0.4 M and 0.6 M. The changes in electrolyte were done to observe the effect on electrolyte associated losses to the total voltage (see Section 2.3). This change in electrolyte and other operational parameters are summarized in Appendix A, Table A.2.

2.2.3. Start-up and operation

Before start-up, the GAC packed reactor was "charged" by applying a current density of about −69 A $m^{-3}{}_{BES}$, until a cathode potential of −0.53 V vs. Ag/AgCl was reached. This target potential was chosen once it resulted in methane production in previous laboratory scale work on methane producing BES. [16]

After inoculation, at day 0, the set-up was started by applying a fixed current density of −6 A $m^{-3}{}_{BES}$ (normalized to the BES volume (0.017 m^3)). This was done by using a potentiostat (HP 96 – 20, Bank Elektronik - Intelligent Controls GmbH, Pohlheim) and the applied current density was confirmed by using an online data logging system (Labview).

After start-up the current density was increased in a step-wise approach in order to increase the methane production rates throughout the 470 day operation of the BES, with a maximum applied current density of −122 A $m^{-3}{}_{BES}$ from day 444 to day 470. These changes in current density in addition to changes in electrolyte composition and interchange strategy after start-up are summarized in Appendix A, Table A.2.

Throughout the operation of the reactor, vitamin, minerals, ammonium and water were added regularly. Moreover, the temperature of the reactor was maintained at around 30 °C by using a water bath (with a set point of 40 °C) that was circulated over water jackets that were placed around the interchange vessel and the bubble column.

2.3. Performance analysis

The bubble column gas outflow was sampled twice per week to quantify carbon dioxide, methane, nitrogen, oxygen and hydrogen content using gas chromatography. [16] Taking into account the percentage of methane in the vent gas and the amount of gas produced, calculated with a gas flow meter (μ Flow unit, Bioprocess Control, Sweden), the methane production rate was calculated. From day 98 onward, a small amount of methane was detected in the outflow of the interchange vessel, hence the amount of methane in the outflow of the interchange vessel was also quantified. In this paper, the total methane production rate was normalized by the total volume of the BES (0.017 m^3).

The resulting cathode potential and anode potential were monitored every minute using an online data logging collection system (Labview). Furthermore, the cathode potential, anode potential and cell voltage were measured manually with a multimeter twice per week. pH (PHM210, MeterLab®), conductivity (HQ440d multi, Hach), and the ammonium content (Hach Lange (LCK305), Hach) of the electrolyte were measured once or twice a week by sampling the inlet to the cathode and anode chambers.

2.3.1. Performance indicators

Methane production rate (1), faradaic efficiency (2), voltage efficiency (3), and energy efficiency (4) were calculated according to previous work, [16] and as shown below.

$$Methane\ production\ rate\ (NL\,m^{-3}\,d^{-1}) = \frac{CH_4 \times gas\ flow\ rate}{100 \times V_{BES}} \tag{1}$$

where CH_4 (in %) is the methane concentration in the vent gas which is quantified by gas chromatography, gas flow rate (in NL d^{-1}) is the combination of the amount of gas in normalized volume (NL) and the time between samples (days) which are both quantified using a flow meter, and V_{BES} (in m^3) is the total volume of the BES, including anode and cathode chamber.

$$Faradaic\ efficiency(\%) = \frac{CH_4 \times gas\ flow \times P}{100 \times R \times T} \times \frac{8 \times F}{I} \tag{2}$$

$$Voltage\ efficiency(\%) = \frac{\Delta G_{CH_4}}{cell\ voltage \times 8 \times F} \tag{3}$$

$$Energy\ efficiency(\%) = \frac{CH_4 \times \Delta G_{CH_4}}{I \times cell\ voltage} \tag{4}$$

where CH_4 produced is in mol_{CH_4}, gas flow is in NL (see above), P is the atmospheric pressure (101.33 kPa), R is the ideal gas constant (8.31 kPa L mol^{-1} K^{-1}), T is the temperature (in K), 8 is the fraction of electrons needed per molecule of CH_4 (in mol_{e^-} mol_{CH_4-1}), F is the Faraday constant (96 485 C $mol_{e^-}{}^{-1}$), I (in C) is the amount of current applied/fixed in the system (in A) times the amount of time between sampling days (in s), ΔG_{CH_4} is the energy density per mole of CH_4 (890.4×10^3 J $mol_{CH_4}{}^{-1}$), and cell voltage (in V) is the experimental cell voltage measured with the multimeter.

2.3.2. Loss distribution

The overall voltage losses can be distributed over (1) cathode overpotential, (2) anode overpotential, (3) pH losses, (4) ionic losses, and (5) other (transport) losses. The contribution of these different losses to the overall energy efficiency (in specific, voltage efficiency) were calculated according to literature. [20] The only difference being that the pH loss was calculated separately from the cathode overpotential and anode overpotential, in comparison to the referred literature. These calculations are shown in Appendix B.

3. Results

3.1. Performance of a 17 L methane producing BES

The 17 L methane producing BES was operated for 470 days with a step wise increase in current density resulting in a proportional step wise increase in methane production rate throughout the operational time, which is shown in Fig. 3. In specific, the current density was increased step wise from −6 A m^{-3} to −122 A m^{-3}, and the resulting methane production rates increased between from 10 NL m^{-3} d^{-1} to 280 NL m^{-3} d^{-1}. Moreover, the electrolyte changes (represented with the vertical lines in Fig. 3) had no clear influence on methane production rates since stable rates were recorded from day 80 to 220 when 0.2 M bicarbonate was added and subsequently bicarbonate concentrations were increased up to 0.6 M.

The resulting faradaic efficiency of the BES set-up ranged between 80% and 100% for the majority of the experimental run, with exception for a few data points after day 51 which corresponds to the timing when the electrolyte interchange strategy was started, and before losses of methane were detected in the outflow of the interchange vessel (see Section 2.1). The trend in faradaic efficiency over time showed no clear influence of changing electrolyte or current density.

The resulting voltage efficiency decreased from around 50% to around 30% with increasing current density when operating under standard (50 mM phosphate) electrolyte (up to day 100). As a result, the energy efficiency also decreased from 40% to 20%. In contrast, at fixed current density, the voltage efficiency increased when the electrolyte was changed by adding Na^+/K^+ bicarbonate up to a concentration of 0.2 M at day 100. Voltage efficiency further increased with increasing bicarbonate concentration of the electrolyte (up to 0.6 M from day 183 onward). The resulting energy efficiency increased to values above 40% from day 130 onward. At operation under 0.6 M electrolyte, a further increase in current density (from day 250) did not lead to a clear influence in the voltage efficiency in comparison to operation under standard electrolyte. As a result, a stable performance with resulting energy efficiency around 45%–50% was observed with operation under 0.6 M electrolyte and increasing current density up to −122 A m^{-3}. The different components influencing voltage losses and energy efficiency are further discussed in the following section.

Although a stable performance was observed at operation under 0.6 M bicarbonate electrolyte, a maximum methane production rate of 280 NL m^{-3} d^{-1} is 2× to 10× lower than reported in laboratory scale methane producing biocathodes with GAC as cathode material (433 L m^{-3} d^{-1}, [16] and 2150 L m^{-3} d^{-1} [18]). Nevertheless, it is likely that higher methane production rates could be reached in this BES with further increase in current density, since the results in Fig. 3 do not yet suggest a limiting performance in terms of faradaic and energy efficiency. In Section 4.1 the performance of this up-scaled BES is compared to other up-scaling designs in literature. Additional performance details of the BES are given in Appendix C, in Figs. C.5, C.6 and C.7.

3.2. Distribution of losses in a scale up methane producing BES

To better understand the influence of different electrolyte compositions, applied current densities, and anode electrode sizes on the overall voltage efficiency, the components of the overall voltage loss in the BES (calculated according to Appendix B) were studied. In Fig. 4 these components, (1) cathode overpotential, (2) anode overpotential, (3) pH losses, (4) ionic losses, and (5) other (transport) losses (Rest) are summarized. Note that for condition A and B the anode overpotential (2) and other transport losses (5) are not separated due to the fact that during this time there was no reference electrode at the anode, thus the anode potential (and overpotential) could not be measured.

Comparing A and B shows that changing from the standard 0.05 M phosphate electrolyte (A) to 0.2 M Na^+/K^+ bicarbonate electrolyte (B) resulted in a decrease of the overall losses from approximately 80 mΩ m^3 to approximately 75 mΩ m^3, at similar current densities. Furthermore, during the operation under 0.2 M electrolyte the pH loss became slightly negative and the ionic losses also decreased, in comparison to standard electrolyte. Overall, the largest contributor to total resistance was for both conditions the combination of anode overpotential and transport losses (that could not be separated due to absence of anode reference electrode).

Further increasing the alkalinity to 0.4 M and 0.6 M, at similar current densities, (C and D) also led to lower overall losses, although the difference was less pronounced. In C and D, the contributions of anode overpotential and transport losses could be measured separately, revealing that for these conditions the anode overpotential was the

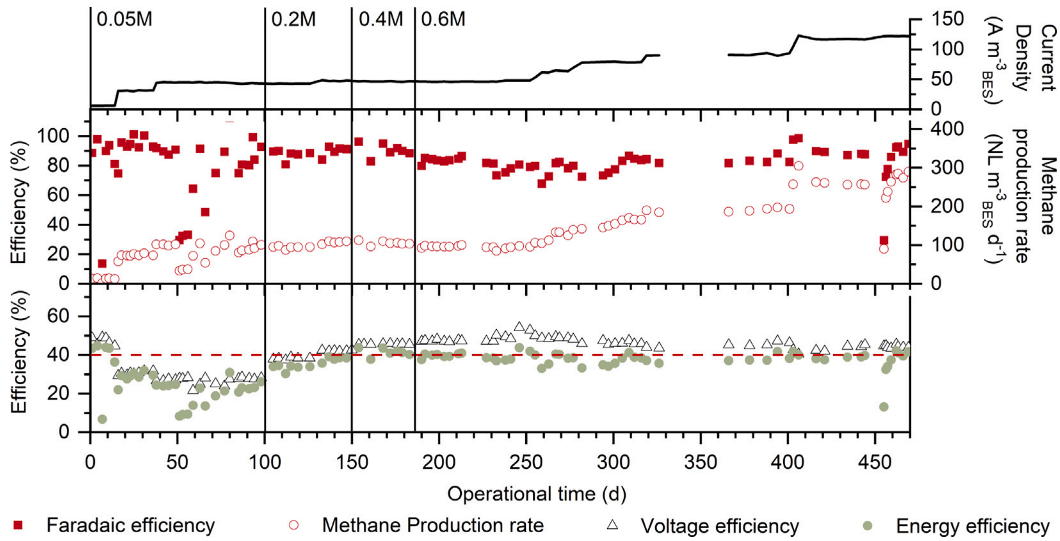

Fig. 3. Methane production rate (middle, right axis), faradaic efficiency towards methane (middle, left axis), voltage efficiency (bottom) and energy efficiency (bottom) throughout the operational time of the scale up methane producing BES. The control strategy, applied current density, is shown on top. Vertical lines represent the change from operation with standard electrolyte (0.05 M phosphate) to 0.2 M Na^+/K^+ bicarbonate electrolyte, and subsequently to 0.4 M Na^+/K^+ bicarbonate electrolyte, and subsequently to 0.6 M Na^+/K^+ bicarbonate electrolyte.

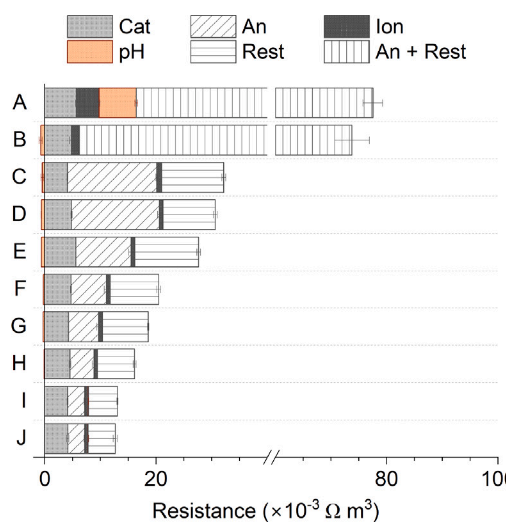

	Electrolyte (M)	Current Density (A m^{-3})	Anode size (m^{-2})
A	0.05	45	0.01
B	0.2	43	0.02
C	0.4	46	0.02
D	0.6	46	0.05
E	0.6	47	0.09
F	0.6	65	0.09
G	0.6	79	0.09
H	0.6	92	0.09
I	0.6	117	0.09
J	0.6	122	0.09

Fig. 4. Distribution of voltage losses normalized by current density, in Ω m^3_{BES} at different operational conditions. The different operational conditions are summarized to the right of the graph including electrolyte composition (in M), applied current (in A m^{-3}), and anode size (in m^2). The observed total cell voltage is: (A) −4.35 V, (B) −2.93 V, (C) −1.47 V, (D) −1.38 V, (E) −1.28 V, (F) −1.31 V, (G) −1.44 V, (H) −1.47 V, (I) −1.53 V, (J) −1.55 V. The sampling days were: (A) days 38–49, (B) days 108–126, (C) days 160–183, (D) days 190–211, (E) days 233–241, (F) days 263–277, (G) days 301–316, (H) days 366–401, (I) days 434–444, (J) days 456–469. Note that there is an axis break between 40 to 60 mΩ m^3 for better visualization.

biggest contributor to the overall loss, followed by the other transport losses, and then the cathode overpotential.

Comparing D and E, when increasing the anode surface area from 0.02 m^2 to 0.05 m^2 the anode overpotential decreased drastically, leading to losses similar to the transport losses. A further increase in anode surface area to 0.09 m^2 (F) led to an even further decrease in the anode overpotential related losses. These were accompanied by a reduction of the total loss as well. Hence, the size of the anode electrode can potentially further be increased to further reduce the total losses and increase the voltage efficiency. However, this would also mean increased costs.

Between F and J the current density was step-wise increased from −65 to −122 A m^{-3} and the total voltage loss (in V) also increased. However, between F and I the resulting contribution of the anode overpotential and other transport losses decreased significantly, thus decreasing the total losses normalized by current density. Between I and J, the contribution of the losses did not change much, meaning that the losses increased proportionally to the increase in current density, suggesting that this would be the case if further increasing the current density.

Overall, the contribution of ionic losses was low and the contribution of transport losses was the highest (when normalized by applied current density). Both ionic and transport losses were considerably reduced by increasing the bicarbonate concentration of the electrolyte. The contribution of anode overpotential, although substantial at first (around 16 mΩ m^3_{BES}), was successfully reduced with increasing anode size. Moreover, when increasing current density, both anode and other transport losses increased but not as much as the increase in

Table 1
Performance overview of scale up BES for power-to-methane application. NR is used for not reported data.

BES volume (L)	Area current collector (m^2)	Current density ($A\ m^{-2}$)	Current density ($A\ m^{-3}$)	Methane prod. rate (NL $m^{-3}{}_{BES}$ d^{-1})	Fara- daic eff. (%)	Cell voltage (V)	Volta- ge eff. (%)	Ener- gy eff. (%)	Ref.
50	3.00	8×10^{-2}	5	5	114	−3.1	NR	27	[11]
45	0.05	22	18	49	96	NR	NR	43	[12]
45	0.05	44	36	83	92	NR	NR	40	[12]
45	0.05	111	91	116	46	NR	NR	30	[12]
20	0.03	120	197	521	95	−6.5	NR	20	[13]
20	0.03	180	295	757	45	−8.0	NR	14	[13]
17	0.31	6	118	280	88	−2.6	45	40	This

applied current density, therefore their overall relative contribution (normalized by applied current density) decreased. In contrast, the relative contribution of cathode overpotential to the overall losses remained fairly stable for all tested conditions, suggesting a linear relationship between cathode overpotential and applied current density, where e.g.doubling the current density would result in double the losses at the cathode. Therefore, out of all components of this BES design, the cathode overpotential remains the most limiting. A cathode overpotential of 5 mΩ $m^3{}_{BES}$ is equal to approximately 0.1 Ω $m^2{}_{cathode\ current\ collector}$. In comparison, at the laboratory scale the cathode overpotential of bioelectrochemical systems converting CO_2 into other products (including acetate and volatile fatty acids) showed lower ranges between 0.004 and 0.07 Ω m^2. [21] Therefore, there is still room to improve on the contribution of the cathode overpotential at a larger scale.

In this study the minimum total loss was equal to 0.26 Ω $m^2{}_{current\ collector}$, which sits on the high end of the range found in the previously mentioned study on laboratory scale (0.04 and 0.2 Ω m^2). [21] Therefore, the design in this work shows promising results, since a larger scale BES performs similarly to some laboratory scale BESs in terms of losses. However, similarly to the cathode overpotential, there is still room to improve the overall design in a way that the total losses in the larger scale decrease up to values similar to the best performing laboratory scale BES designs (yielding total losses of 0.04 Ω m^2).

4. Discussion

4.1. Performance of other methane producing BES scale up designs

In Table 1, the performance of scale up methane producing BESs, with cell volumes equal to or above 17 L, is summarized. In contrast to our design, the summarized work includes, a 50 L tubular reactor with 3 m^2 carbon laying cathode, [11] a 45 L moving bed reactor with fixed 0.05 m^2 stainless steel mesh cathode, [12] and a 20 L continuous stirred tank (CSTR) with an inserted tubular BES of 0.35 L with a 0.03 m^2 stainless steel mesh cathode. [13] For the last case the 20 L volume is taken into account in the table because it is assumed that the conversion of CO_2 into methane takes place in the entire volume of the CSTR. For a schematic representation of each design please check the referred work.

The 50 L tubular cathode was the first study to run a scale up BES with pure culture *Methanococcus maripaludis*. [11] The reported faradaic efficiency averaged above 100%. Authors suggested that methane formation occurred from additional electron sources but did not describe which. Although the resulting energy efficiency ranged around 27%, low methane production rates were reported, 5.2 L_{CH_4} m^{-3} d^{-1}, due to the resulting low current density at an applied cell voltage of −3.1 V.

In the moving bed reactor type, an energy efficiency up to 43% was observed, [12] slightly higher than in this work, 40%. However, this occurred at the expense of lower methane production rates, 49 L_{CH_4} m^{-3} d^{-1}, in comparison to this work, 280 L_{CH_4} m^{-3} d^{-1}. Further increasing the current density, leading to higher methane production rates such as 116 L_{CH_4} m^{-3} d^{-1}, consequently led to a decrease in energy efficiency to 30% and faradaic efficiency to 46%, with formation of by-products such as hydrogen and acetate.

The tubular BES inserted in the continuous stirred tank showed overall best rates, reporting methane production rates of 521 and 757 L_{CH_4} m^{-3} d^{-1}. [13] However, this came at the expense of large voltages, −6.5 V and −8.0 V, respectively. Hence, the resulting energy efficiency was comparatively low, up to 20%. Larger voltage most probably resulted from hydrogen mediated methanogenesis, once hydrogen was detected as a by-product, and the distance between the reactive surface area of the cathode and reaction sight in the CSTR can be large.

The larger trade off between energy efficiency and rates reported in the previous two studies, [12,13] in contrast to this work, are probably a consequence of ten times smaller cathode current collector surface area (see Table 1).

4.2. Challenges of the current scale up BES design

4.2.1. Larger losses in comparison to laboratory scale BES

The losses of this scale up BES rest among the high estimates for laboratory scale BES for CO_2 conversion. The main contributors in this design were losses associated to transport over the membrane and cathode overpotential. Moreover, the anode overpotential was initially high, but was decreased by increasing its surface area up to 0.09 m^2. Similarly, other aspects of the reactor configurations might need to be adjusted in order to decrease the losses associated to cathode overpotential and transport.

As to decrease the transport losses, the distance between the electrodes and between the electrodes and the membrane should be minimized. To do so, the diameter of the tubular membrane could be decreased for a better fit around the anode, whilst maintaining the area of the membrane by increasing the height of the reactor. Optionally, bringing the cathode current collector closer to the center as well, and creating a thinner GAC bed can help reduce transport resistance that might occur over the depth of the GAC bed. However, the local conditions at the cathode are unknown, which limits our understanding of how cathode overpotential can be decreased. In a study on chain elongation biocathodes, H_2, pH and ORP local measurements were made with microsensors in order to identify rate limiting factors present at the biocathode. [22] In the same study, once gradients were observed the process conditions were adjusted to optimize reaction rates. Similarly, conducting local measurements at methane producing GAC based biocathodes might give indications of what needs to be avoided when scaling up, and what can possibly be the cause for larger cathode overpotentials in the scale up, e.g. vertical gradients in height or horizontal gradients in depth.

4.2.2. Maintaining conductivity during operation with haloalkaline electrolyte

Although operation under haloalkaline led to a lower sum of voltage losses, it can also lead to significant changes in conductivity of the anolyte and catholyte, once cations travel from the anode to the cathode as a consequence of the electron flow (from the anode to the cathode). In order to avoid changing conductivity in time, an "interchange strategy" was used to mix the catholyte and the anolyte, and as a result a similar conductivity and pH of recirculating anolyte and catholyte was maintained (see Appendix C, Fig. C.7). However, using the interchange vessel, to mix the catholyte and analyte, led to CH_4 losses via the gas outlet of the interchange vessel, which was continuously sparged with N_2 to maintain low oxygen conditions. Therefore, either the use of the interchange strategy has to be minimized or another strategy has to be implemented. A possible alternative strategy could be feeding the bleed of the cathode recirculation to the anode recirculation and vice versa, without using the interchange vessel.

4.3. Opportunities of the current scale up BES design

4.3.1. Long term stable performance

Overall, the 17 L scale up methane producing BES was operated for 470 days at stable performance, with energy efficiency above 35%. After the start-up period of 70 days the energy efficiency remained around and above 40%. At 40% energy efficiency, large rates of methane production up to 280 NL $m^{-3}{}_{BES}$ d^{-1} were reached. Larger rates found in literature on scale up methane producing BES were only reached at the expense of energy efficiency (below 20%). Moreover, the limiting rates of the scale up were not tested. Since, (1) faradaic efficiency remained high throughout the operation, (2) no H_2 was detected in the outlet gas, and (3) it is possible that larger rates of methane production can still be reached with this design.

4.3.2. CO_2 absorption

In this scale up BES the catholyte was recirculated between the cathode chamber and a bubble column (more details are provided in the Methods section). In this way, CO_2 was sparged in the bubble column and the liquid was recirculated to the cathode, where dissolved CO_2 in the liquid phase was converted to CH_4, which was then recirculated back to the bubble column, where the CH_4 was stripped from the electrolyte and replaced by CO_2, while the CH_4 could escape via the gas outlet of the bubble column. The use of a haloalkaline electrolyte allows more CO_2 to be dissolved, in comparison to standard electrolyte. Moreover, it buffers pH changes resulting from dissolving and converting CO_2, allowing a more stable environment for microorganisms (in terms of pH). Here, by setting the CO_2 inflow rate at approximately 5.5 NL d^{-1}, the CH_4 concentration in the gas outlet reached 75% when operating at –125 A m^{-3} and with 0.6 M Na^+/K^+ bicarbonate electrolyte (see Appendix C, Fig. C.6). CO_2 absorption columns are commonly implemented in biogas upgrading technologies at industrial scale, and yield CH_4 concentrations around 98%. [23] Therefore, implementing commercially available equipment should further improve gas-to-liquid interactions, thus improving performance and the resulting CH_4 content. Therefore, the CO_2 absorption at an industrial scale is not perceived as an issue/bottleneck. Moreover, currently implemented biogas upgrading technologies rely on physical removal of CO_2 from biogas, rather than the conversion of CO_2. The removed CO_2 is more often than not released back to the atmosphere. Utilizing methane producing BES to treat these CO_2-rich streams presents a promising initial application. This approach not only decreases the amount of CO_2 released to the atmosphere, but also enhances the production of biomethane.

4.3.3. Economic assessment

At this stage, a techno-economic assessment of the scalable design is crucial in order to understand how competitive this scale up methane producing BES is in comparison to other power-to-gas alternatives, and other electricity storage alternatives. As sources of revenue, the techno-economic assessment should take into account, (1) the value of (bio)methane as an end product, (2) the value of using CO_2-rich streams which are currently polluting the environment and (3) the value of supporting the function of electricity storage infrastructure, e.g. by taking up electricity from the grid when its production surpasses demand. An additional source of revenue can come from the O_2 produced at the anode, which can be of interest for chemical synthesis or medicine (if highly pure O_2 streams can be achieved). As sources of expenditures, the assessment should take into account both capital expenditures and operational expenditures. In general, operational expenditures are expected to be much lower in comparison to capital ones, once the former mainly accounts for electricity, CO_2 streams and maintenance with water, bicarbonate, and nutrients. Moreover, understanding the durability of the electrode materials, the membrane and other system components (e.g. reference electrodes) is highly important in order to estimate the contribution of repair and maintenance costs to the operational expenditures. Similar economic assessments have been done on laboratory scale BES for CO_2 reduction to methane, [24] and short chain fatty acids. [25] However, the assessment itself highly depends on, e.g., chosen materials, reactor design and resulting performance. With this said, integrating the previously referred techno-economic assessments to the results shown in this paper is an important step towards understanding the technological readiness level of this novel design for methane producing BES.

5. Conclusion

The galvanostatic controlled 17 L scale up BES design as described in this paper resulted in the largest methane production rates of 280 L m^{-3} d^{-1} at an energy efficiency of 40%, in comparison to other reactor designs with volumes above 17 L. Larger rates have been reported in literature but only at the expense of energy efficiency. Nevertheless, the limiting rates of this BES design were not yet tested and it is likely that higher rates can be reached. Moreover, the transport losses across the membrane accounted for the majority of the voltage losses in this design. Thus, decreasing the distance between the anode electrode and the membrane, whilst maintaining the area of the membrane, is suggested to further improve the energy efficiency of the current design. Overall, this work shows that the current design is promising for scaling up bioelectrochemical systems in general.

CRediT authorship contribution statement

Micaela Brandão Lavender: Writing – review & editing, Writing – original draft, Supervision, Formal analysis, Conceptualization. **Jos Steller:** Writing – review & editing, Investigation, Formal analysis, Conceptualization. **Dandan Liu:** Writing – review & editing, Supervision, Investigation, Conceptualization. **Rieks de Rink:** Writing – review & editing, Conceptualization. **Shiba Tofik:** Investigation, Formal analysis. **Annemiek ter Heijne:** Writing – review & editing, Supervision.

Declaration of competing interest

All authors declare that they have no known competing financial interests or personal relationships that could have appeared to influence the work reported in this paper.

Acknowledgments

We would like to acknowledge Shell Global Solutions International B.V. and Paqell B.V. for funding the research. We would like to thank Jan Klok for the scientific contribution to this work. We would like to thank Nicolas Tsesmetzis for the fruitful discussions. Additionally, we would like to acknowledge Vinnie de Wilde, Michiel van den Broek and Bert Willemsen for helping with the design and construction of the experimental set-up.

Appendix A. Operational details of the 17 L scale up methane producing BES

See Table A.2.

Table A.2
Details of the operation of the scale up methane producing BES throughout the 470 days of operation. At day 0, the BES was controlled at −6 A m^{-3}, at day 14 the current density was increased to −31 A m^{-3} and at day 36 it was again increased to −43 A m^{-3}. At around −43 A m^{-3}, the electrolyte composition was changed three times, from standard electrolyte to 0.2 M haloalkaline electrolyte on day 100, to 0.4 M haloalkaline electrolyte on day 150 and to 0.6 M haloalkaline electrolyte on day 183. At 0.6 M haloalkaline electrolyte and from day 233 onward a step-wise increase in current density was performed with a maximum applied of −122 A m^{-3} at day 444. The interchange strategy was not used up to day 51.

Days of operation	Applied current density	Electrolyte composition	Interchange strategy
0–14	−6 A m^{-3}	0.05 M phosphate	OFF
14–36	−31 A m^{-3}	0.05 M phosphate	OFF
36–51	−43 A m^{-3}	0.05 M phosphate	OFF
51–100	−43 A m^{-3}	0.05 M phosphate	P3 and P5 on
100–150	−43 to −48 A m^{-3}	0.2 M bicarbonate	P3 and P5 on
150–183	−46 A m^{-3}	0.4 M bicarbonate	P3 and P5 on
183–233	−46 A m^{-3}	0.6 M bicarbonate	P3 and P5 on
233–277	−48 to −69 A m^{-3}	0.6 M bicarbonate	P3 and P5 on
277–400	−80 to −90 A m^{-3}	0.6 M bicarbonate	P3 and P5 on
400–444	−105 to −117 A m^{-3}	0.6 M bicarbonate	P3 and P5 on
444–470	−122 A m^{-3}	0.6 M bicarbonate	P3 and P5 on

Appendix B. Equations representing the detailed calculations of the different losses/resistances contributing to the cell voltage of the BES

The resulting cell voltage is composed of the equilibrium voltage (E_{eq}) and the following losses: the cathode overpotential (E_{Cat}), the anode overpotential (E_{An}), the pH associated resistances (E_{pH}), the electrolyte resistances (E_{Ion}) and the other transport losses (E_T). All calculated as shown in Eqs. (B.1) to (B.6), respectively.

The ratio between each component (Eqs. (B.1) to (B.6)) (in V) and the current density ($I_{density}$) (in A m$^{-3}{}_{BES}$) is equal to the resistance associated to each component, in Ohm m^3, as shown in Eq. (B.7).

$$E_{eq} = E_{Cat\,theoretical} - E_{An\,theoretical} \tag{B.1}$$

$$E_{Cat} = E_{Cat\,theoretical} - E_{Cat\,measured} \tag{B.2}$$

$$E_{An} = E_{An\,measured} - E_{An\,theoretical} \tag{B.3}$$

Where $E_{Cat_{theoretical}}$ and $E_{An_{theoretical}}$ are the expected cathode and anode potentials (in V) at pH 7 and based on the experimental conditions (temperature, reactants concentrations and products concentrations), and $E_{Cat_{measured}}$ and $E_{An_{measured}}$ are the measured potentials (in V).

$$E_{\Delta pH} = \frac{RT}{F} \times \ln(10^{(pH_{Cathode} - pH_{Anode})}) \tag{B.4}$$

Where R is the ideal gas constant (8.31 kPa L mol^{-1} K^{-1}), T is the temperature (in K) and F is the Faraday constant (96 485 C mol$_{e^-}{}^{-1}$).

$$E_{ion} = I_{ions} \times (\frac{d_{An}}{2A_{CC}\sigma_{An}} + \frac{d_{Cat}}{2A_{CC}\sigma_{Cat}}) \tag{B.5}$$

Where I_{Ions} is the flow of ions through the electrolyte (in A m^{-3}, same as the current density), d_{An} and d_{Cat} is the distance between the respective electrode material and the membrane, and σ_{An} and σ_{Cat} is the conductivity of the respective electrolyte (in S m^{-1}).

$$E_T = E_{cell} - (E_{eq} - E_{Cat} - E_{An} - E_{ion}) \tag{B.6}$$

$$R_X = \frac{E_X}{I_{density}} \tag{B.7}$$

Appendix C. Performance details of the 17 L scale up methane producing BES

See Figs. C.5–C.7.

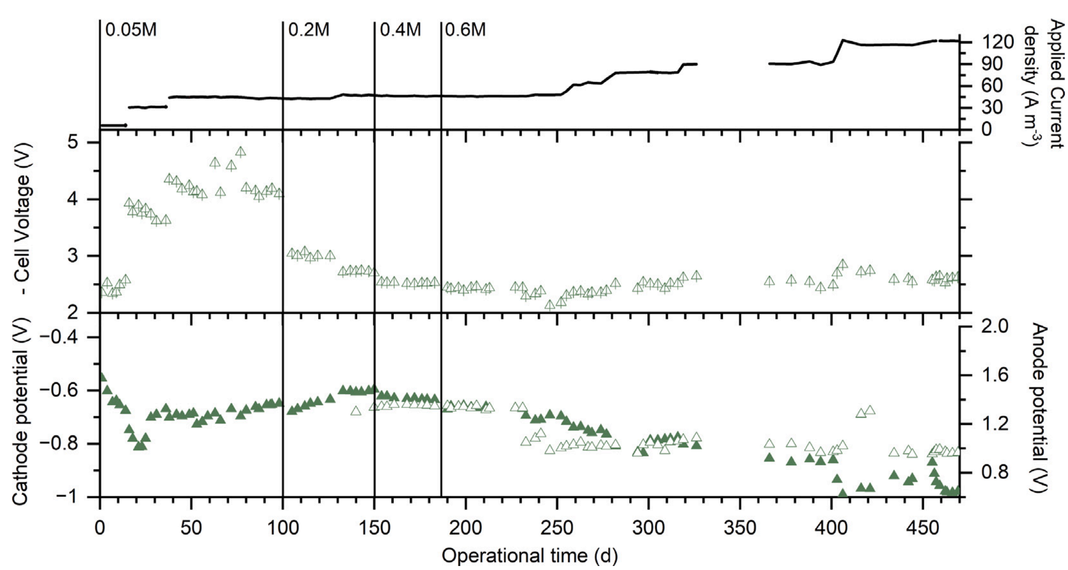

Fig. C.5. Plot of cell voltage (middle), cathode potential (full triangles, bottom) and anode potential (empty triangles, bottom), throughout the operational time of B1. The control strategy, applied current density, is also plotted for reference (top). Vertical lines represent the change in electrolyte.

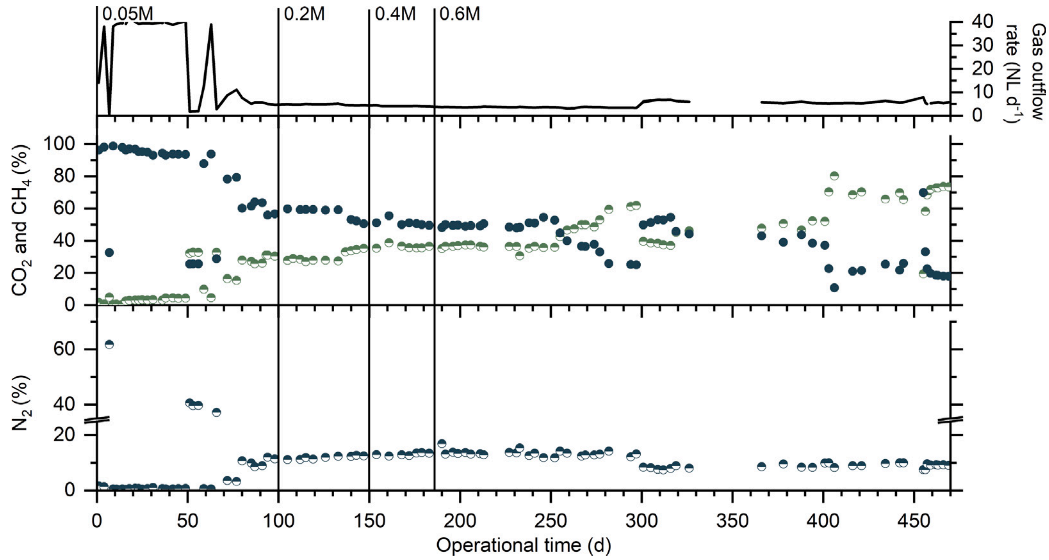

Fig. C.6. Plot of the composition of the outflow gas from the headspace of the bubble column, including CO_2 (in V%) (dark full circles, middle), CH_4 (in V%) (green half circles, middle), and N_2 (in V%) (dark half circles, bottom). The flow rate of the gas outflow is plotted at the top. Vertical lines represent the change in electrolyte. (For interpretation of the references to color in this figure legend, the reader is referred to the web version of this article.)

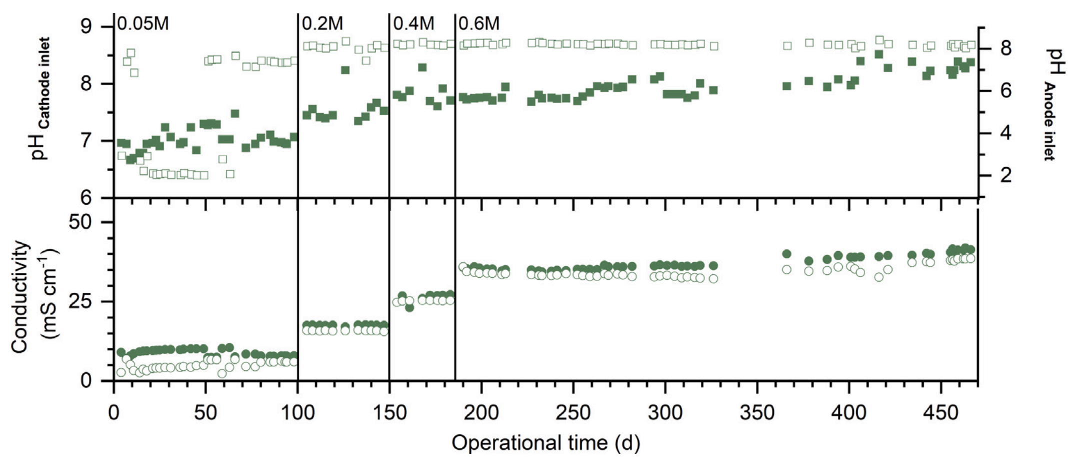

Fig. C.7. Plot of the pH (top) and conductivity (bottom) of the electrolyte at the inlet of the cathode (green full squares and circles, respectively), and at the inlet of the anode (empty squares and circles, respectively). Vertical lines represent the change in electrolyte. (For interpretation of the references to color in this figure legend, the reader is referred to the web version of this article.)

Data availability

The data that supports the findings of this study will be made available at 4TU Research Data repository.

References

[1] IRENA, World energy transitions outlook: Executive summary and introduction, 2023, https://www.irena.org/Digital-Report/World-Energy-Transitions-Outlook-2023.

[2] R.M. Alonso, M.I. San-Martín, R. Mateos, A. Morán, A. Escapa, Scale-up of bioelectrochemical systems for energy valorization of waste streams, in: Microbial Electrochemical Technologies, CRC Press, 2020, pp. 447–459.

[3] A. Janicek, Y. Fan, H. Liu, Design of microbial fuel cells for practical application: a review and analysis of scale-up studies, Biofuels 5 (1) (2014) 79–92.

[4] D.A. Jadhav, S.-G. Park, S. Pandit, E. Yang, M.A. Abdelkareem, J.-K. Jang, K.-J. Chae, Scalability of microbial electrochemical technologies: Applications and challenges, Bioresour. Technol. 345 (2022) 126498.

[5] F. Enzmann, M. Stöckl, A.-P. Zeng, D. Holtmann, Same but different–scale up and numbering up in electrobiotechnology and photobiotechnology, Eng. Life Sci. 19 (2) (2019) 121–132.

[6] A.-J. Wang, H.-C. Wang, H.-Y. Cheng, B. Liang, W.-Z. Liu, J.-L. Han, B. Zhang, S.-S. Wang, Electrochemistry-stimulated environmental bioremediation: Development of applicable modular electrode and system scale-up, Environ. Sci. Ecotechnol. 3 (2020) 100050.

[7] H. Hiegemann, D. Herzer, E. Nettmann, M. Lübken, P. Schulte, K.-G. Schmelz, S. Gredigk-Hoffmann, M. Wichern, An integrated 45 l pilot microbial fuel cell system at a full-scale wastewater treatment plant, Bioresour. Technol. 218 (2016) 115–122.

[8] P. Liang, R. Duan, Y. Jiang, X. Zhang, Y. Qiu, X. Huang, One-year operation of 1000-l modularized microbial fuel cell for municipal wastewater treatment, Water Res. 141 (2018) 1–8.

[9] L. Singh, A.G. Miller, L. Wang, H. Liu, Scaling-up up-flow microbial electrolysis cells with a compact electrode configuration for continuous hydrogen production, Bioresour. Technol. 331 (2021) 125030.

[10] E.S. Heidrich, S.R. Edwards, J. Dolfing, S.E. Cotterill, T.P. Curtis, Performance of a pilot scale microbial electrolysis cell fed on domestic wastewater at ambient temperatures for a 12 month period, Bioresour. Technol. 173 (2014) 87–95.

[11] F. Enzmann, D. Holtmann, Rational scale-up of a methane producing bioelectrochemical reactor to 50 L pilot scale, Chem. Eng. Sci. 207 (2019) 1148–1158.

[12] W. Cai, K. Cui, Z. Liu, X. Jin, Q. Chen, K. Guo, Y. Wang, An electrolytic-hydrogen-fed moving bed biofilm reactor for efficient microbial electrosynthesis of methane from CO2, Chem. Eng. J. 428 (2022) 132093.

[13] G. Shang, K. Cui, W. Cai, X. Hu, P. Jin, K. Guo, A 20 L electrochemical continuous stirred-tank reactor for high rate microbial electrosynthesis of methane from CO2, Chem. Eng. J. 451 (2023) 138898.
[14] A. Ceballos-Escalera, D. Molognoni, P. Bosch-Jimenez, M. Shahparasti, S. Bouchakour, A. Luna, A. Guisasola, E. Borràs, M. Della Pirriera, Bioelectrochemical systems for energy storage: A scaled-up power-to-gas approach, Appl. Energy 260 (2020) 114138.
[15] M. Kim, S. Li, Y.E. Song, D.-Y. Lee, J.R. Kim, Electrode-attached cell-driven biogas upgrading of anaerobic digestion effluent CO2 to CH4 using a microbial electrosynthesis cell, Chem. Eng. J. 446 (2022) 137079.
[16] M.B. Lavender, S. Pang, D. Liu, L. Jourdin, A. Ter Heijne, Reduced overpotential of methane-producing biocathodes: Effect of current and electrode storage capacity, Bioresour. Technol. 347 (2022) 126650.
[17] A.-J. Wang, D. Cui, H.-Y. Cheng, Y.-Q. Guo, F.-Y. Kong, N.-Q. Ren, W.-M. Wu, A membrane-free, continuously feeding, single chamber up-flow biocatalyzed electrolysis reactor for nitrobenzene reduction, J. Hazard. Mater. 199 (2012) 401–409.
[18] D. Liu, M. Roca-Puigros, F. Geppert, L. Caizán-Juanarena, S.P. Na Ayudthaya, C. Buisman, A. Ter Heijne, Granular carbon-based electrodes as cathodes in methane-producing bioelectrochemical systems, Front. Bioeng. Biotechnol. 6 (2018) 78.
[19] E. Wolin, M. Wolin, R. Wolfe, Formation of methane by bacterial extracts, J. Biol. Chem. 238 (8) (1963) 2882–2886.
[20] T.H. Sleutels, H.V. Hamelers, R.A. Rozendal, C.J. Buisman, Ion transport resistance in microbial electrolysis cells with anion and cation exchange membranes, Int. J. Hydrog. Energy 34 (9) (2009) 3612–3620.
[21] T.H. Sleutels, A. Ter Heijne, C.J. Buisman, H.V. Hamelers, Bioelectrochemical systems: an outlook for practical applications, ChemSusChem 5 (6) (2012) 1012–1019.
[22] S.M. de Smit, J.J. Langedijk, J.H. Bitter, D.P. Strik, Alternating direction of catholyte forced flow-through 3D-electrodes improves start-up time in microbial electrosynthesis at applied high current density, Chem. Eng. J. 464 (2023) 142599.
[23] L.N. Nguyen, J. Kumar, M.T. Vu, J.A. Mohammed, N. Pathak, A.S. Commault, D. Sutherland, J. Zdarta, V.K. Tyagi, L.D. Nghiem, Biomethane production from anaerobic co-digestion at wastewater treatment plants: A critical review on development and innovations in biogas upgrading techniques, Sci. Total Environ. 765 (2021) 142753.
[24] D. Liu, Strategies for Improving Methane Production from CO 2 and Electricity in Bioelectrochemical Systems (Ph.D. thesis), Wageningen University and Research, 2018.
[25] L. Jourdin, J. Sousa, N. van Stralen, D.P. Strik, Techno-economic assessment of microbial electrosynthesis from CO2 and/or organics: An interdisciplinary roadmap towards future research and application, Appl. Energy 279 (2020) 115775.